The Working of the Cup Anemometer

Leif Kristensen, Ole Frost Hansen and Svend Ole Hansen
June 19, 2014

1 Introduction

As formulated by Kristensen (1999) the cup anemometer is probably the most common instrument for measuring the wind speed at places weather observations are routinely carried out. We see them in airports, at wind farms, and at construction sites—and for good reasons. Experience has shown the it is a robust and reliable instrument which can operate unattended for years. Since it is omnidirectional it is easy to install.

The cup anemometer was invented in 1846 by the Irish astronomer Thomas R. Robinson. An interesting account of its history, including forerunners, has been given by Middleton (1969). The first anemometers had four cups. This is reflected in the fact that in German the instrument is known as the "Schalenkreuzanemometer". Also in Danish it is sometimes called "skålkorsanemometer". The building blocks in these languages are "Schale"="skål"="bowl"/"cup" and "Kreuz"="kors"="cross". The last part of the word indicates that the cup anemometer originally has four arms. Robinson believed that, provided friction in the bearing can be neglected, a law of nature implied that the speed of the center of the cup was exactly one third of the wind speed. The wind speed divided by the speed of the cup was called *the factor* f. Although this is not too far from reality, it is by no means true. It reflects, however, the remarkable linearity of the calibration, even for the first versions of the instruments.

A thorough investigation of the cup anemometer by Patterson (1926) revealed that the factor varied between 2 and 3. In fact, he found that it varied not only from instrument to instrument, but also as a function of wind speed for a single instrument, albeit to a lesser degree. This of course means that the calibration cannot be completely linear. His work showed that the linearity is better the larger the ratio of the cup radius to the arm length. Another conclusion from his work was that anemometers with three cups is better than cup with four cups because they respond more readily to changes in wind speed.

In the 1920th the cup-anemometer development had led to an instrument with a calibration which had a calibration which, for all practical purposes, could be considered linear. However, it was noticed that in turbulent wind, the output signal was larger for a particular mean-wind speed than the output from the same instrument exposed to a constant wind speed of the same magnitude in a wind tunnel with little turbulence. This phenomenon was called *overspeeding* and it was ascribed to the asymmetric response to changes in the wind speed: for a cup anemometer to work at all, it must respond more readily to an increase than to a decrease in the wind speed (Kristensen 1993, Kristensen 1999). As a consequence, the time spent above the mean wind becomes larger than the time spent below, with the result that the mean-wind measurement will be to large. To analyze the overspeeding it was necessary to understand the dynamics, i.e. the equation of motion, of the cup anemometer. Schrenk (1929) was, according to Wyngaard (1981), the first to publish a systematic attempt to model the dynamics of the motion of the cup-anemometer rotor. From the point of view that it is not possible to describe the detailed air-flow patterns around a moving cup rotor, this model captured the asymmetry by assigning a larger drag coefficient to the concave than to the convex side of the cup. Much effort was invested in the exploitation of this model to understand overspeeding. No definite conclusion was obtained for four decades. Then Wyngaard et al. (1974) decided to set up a pragmatic, phenomenological model for the equation of motion and for the various wind contributions to the torque on the cup rotor. These contributions were measured in a wind tunnel. The new data were interpreted independently by Kaganov & Yaglom (1976) and Busch & Kristensen (1976). They came to the same

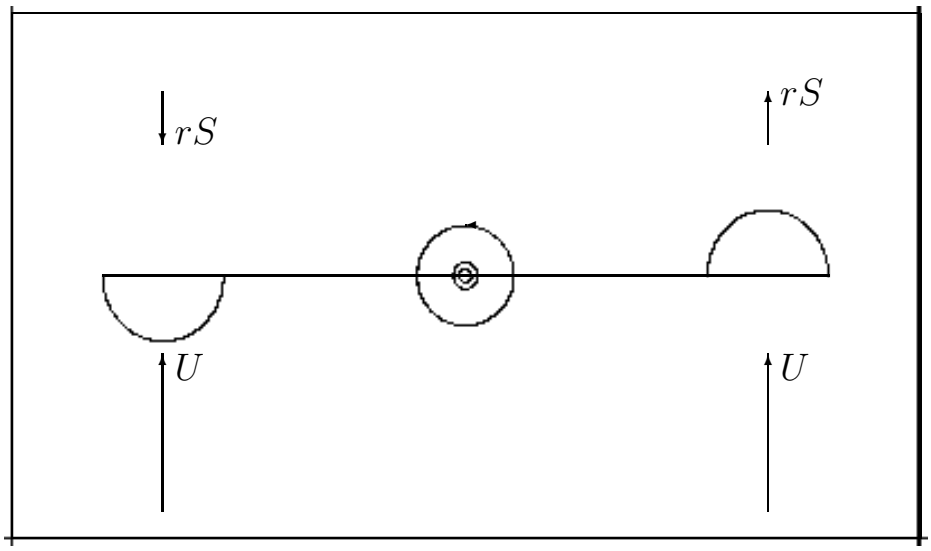

Figure 1: Sketch of the Schrenk model. The rotor has only two cups and shows them in a position where the driving torque has a maximum where the wind speed with the magnitude U blows directly into the concave side to the right and at the back side to the left. The rotor has the angular velocity S so that the speed of the cups is rS, where r is the rotor radius, from the axis to the center of the cups. It is indicated by the arrow on the circle around the axis that in this case the rotation is counterclockwise.

quantitative result for the effect of the asymmetric rotor response. It had to result in a positive bias of the wind speed in a turbulent wind. Both Kaganov & Yaglom (1976) and Wyngaard (1981) have given interesting accounts of the history of overspeeding.

It is generally believed that the overspeeding is entirely due to the asymmetric response. It is true that a slow cup anemometer with a large moment of inertia of the cup rotor overspeeds more than a light and small anemometer with a small moment of inertia. However, a more detailed analysis (Kristensen 1993, Kristensen 1998) shows that in general there are more important contributions to the mean-wind bias one gets in turbulent winds. The most important are related to the fluctuations in the lateral and the vertical velocity components. These biases are both proportional to the corresponding variances, which must be known to correct the mean wind. Further, it is necessary to know the angular response. The ideal angular response is the so-called *cosine response*, which means that the anemometer is sensitive only to the wind component perpendicular to the rotor shaft. If the angular response falls below the cosine response, the anemometer will actually *underspeed*.

The following is a discussion of the operation of the cup anemometer and the sources of the biases of measurements of the mean wind in atmospheric flows with different intensities of turbulence. First, however, we will study some of the properties of the cup anemometer by means of the somewhat oversimplified model by Schrenk (1929).

2 Consequences of the Schrenk Model

Figure 1 shows the cup rotor of the Schrenk anemometer rotating with the angular velocity S. Of course this model is an oversimplification when compared to a real anemometer, but it seems to capture the bulk

properties. The force on each cup is proportional to the square of the relative speed with respect to the wind speed. The factor of proportionality is the product of the density of air ρ, the cross-sectional area A and a dimensionless lift/drag coefficient C which depends on the shape of the cup. The figure shows that this coefficient is larger for the right-hand cup than for the left-hand cup. The lift/drag force on a non-moving body is

$$F = \frac{1}{2} A \rho C U^2. \tag{1}$$

The angular momentum on the rotor can then be written

$$\mathcal{M} = r \times \frac{1}{2} A \rho \left\{ C_+ (U - rS)^2 - C_- (U + rS)^2 \right\}, \tag{2}$$

where C_+ and C_- are the lift/drag coefficients of the right and left cup, respectively. The angular momentum can also be written $\mathcal{M} = I \mathrm{d}S/\mathrm{d}t$ in term of the inertial moment of the rotor$I$ and (2) can be formulated as a differential equation in S

$$\frac{\mathrm{d}S}{\mathrm{d}t} = K_+ (U - rS)^2 - K_- (U + rS)^2, \tag{3}$$

where

$$K_{+/-} = \frac{rA\rho}{2I} C_{+/-} \tag{4}$$

with the dimension of length to the power -2.

When the rotor has a constant angular velocity in a constant wind the left-hand side is zero. This is possible only if

$$K_+ > K_-. \tag{5}$$

Solving

$$0 = K_+ (U - rS)^2 - K_- (U + rS)^2, \tag{6}$$

for S, we obtain the calibration, i.e. S as a function of U,

$$f \equiv \frac{U}{rS} = \frac{\sqrt{K_+} + \sqrt{K_-}}{\sqrt{K_+} - \sqrt{K_-}} \tag{7}$$

in terms of the aforementioned factor f[‡].

[‡]There are actually two solutions to (6), but one must be excluded because it corresponds to the cups having a speed large than the wind.

Now we may analyze the equation of motion (3) in the case where the wind speed is increased by a small amount. Initially S is unchanged, but is not the case for its time derivative. Instead of (3) we now have

$$\frac{\mathrm{d}S}{\mathrm{d}t} = K_+(U + u - rS)^2 - K_-(U + u + rS)^2. \tag{8}$$

To the first order in u this can be written

$$\frac{\mathrm{d}S}{\mathrm{d}t} = \underbrace{K_+(U - rS)^2 - K_-(U + rS)^2}_{=0} + 2\{K_+(U - rS) - K_-(U + rS)\}u + (K_+ - K_-)u^2. \tag{9}$$

Obviously, the first term on the right-hand side is zero by virtue of (6). This means that

$$\sqrt{K_+}(U - rS) = \sqrt{K_-}(U + rS) \tag{10}$$

which, combined with (3), implies

$$K_+(U - rS) > K_-(U + rS). \tag{11}$$

In other words, in the perturbation equation (9) the coefficients to both u and u^2 are positive. The implication is that when u is positive, corresponding to increased wind speed, the angular acceleration $\mathrm{d}S/\mathrm{d}t$ is larger than when u is negative. The rotor picks up speed in response to a wind-speed increase more readily than it brakes at a wind-speed decrease of the same n magnitude. This reveals the source of the overspeeding, but a more realistic physical model is needed to quantify it. We return to that later. First, however, we must discuss the tools we need about velocity turbulence.

The following three section might be considered heavy going, and the reader, not interested in detailed documentation, may get the information needed by skipping to the section 7.

3 Entr'acte: Standard Tools in Turbulence Analysis

We consider a turbulent, statistically homogeneous and stationary velocity field $\widetilde{\boldsymbol{u}}(\boldsymbol{x}, t)$ as a function of position in space $\boldsymbol{x}$ and time t. The mean wind speed U of is considered constant in time and direction and defines one direction in a Cartesian coordinate system. Let this direction be defined by the unit vector $\boldsymbol{i}_1$. The unit vectors $\boldsymbol{i}_2$ and $\boldsymbol{i}_3$ are perpendicular to one another and to $\boldsymbol{i}_1$. These three vectors define our coordinate system. Indication averaging by brackets ($\langle\rangle$) we therefore have

$$\langle\widetilde{\boldsymbol{u}}(\boldsymbol{x}, t)\rangle = U \times \boldsymbol{i}_1. \tag{12}$$

We make a Galilean coordinate transformation with the velocity $U \times \boldsymbol{i}_1$ and assume Taylor's "frozen turbulence" hypothesis[§]. In the new coordinate system the random velocity field $\boldsymbol{u}$ is, informally stated,

[§]In an informal way it states that all (rapid and turbulent) temporal fluctuations at a given point are entirely made up of "stiff" spatial velocity fluctuations which are carried through the point by the mean wind.

not a function of time. The argument t is consequently omitted. In this way Taylor's hypothesis can be formulated

$$\boldsymbol{u}(\boldsymbol{x}) = \widetilde{\boldsymbol{u}}(\boldsymbol{x} - Ut \times \boldsymbol{i}_1, 0) - U \times \boldsymbol{i}_1. \tag{13}$$

It can be written with its three components as

$$\boldsymbol{u}(\boldsymbol{x}) = u_1(\boldsymbol{x})\boldsymbol{i}_1 + u_2(\boldsymbol{x})\boldsymbol{i}_2 + u_3(\boldsymbol{x})\boldsymbol{i}_3, \tag{14}$$

where

$$\boldsymbol{x} = x_1\boldsymbol{i}_1 + x_2\boldsymbol{i}_2 + x_3\boldsymbol{i}_3. \tag{15}$$

We assume incompressibility, i.e.

$$\frac{\partial u_i}{\partial x_i} = 0, \tag{16}$$

using the usual summation convention to expression with doubly occurring indices.

Finally, the velocity field is considered isotropic in the following.

The ensemble averages of the three velocity components u_i are of course zero. The second-order covariances are the elements in the 3×3 tensor

$$R_{ij}(\boldsymbol{r}) = \langle u_i(\boldsymbol{x}) u_j(\boldsymbol{x} + \boldsymbol{r}) \rangle, \qquad \left.\begin{matrix} i \\ j \end{matrix}\right\} = 1, 2, 3 \tag{17}$$

where $\boldsymbol{r}$ is the displacement vector. In addition to homogeneity, i.e. translational invariance, and reflection symmetry we have

$$R_{ij}(\boldsymbol{r}) = R_{ji}(\boldsymbol{r}) = R_{ij}(-\boldsymbol{r}). \tag{18}$$

The three diagonal elements are the auto-covariances. In *isotropic* turbulence there are only the longitudinal and lateral auto-covariances. They are the longitudinal covariance with the velocity components along the displacement vector

$$R_L(r) = R_{11}(r\boldsymbol{i}_1) = R_{22}(r\boldsymbol{i}_2) = R_{33}(r\boldsymbol{i}_3) \tag{19}$$

and the transversal covariance with the velocity components perpendicular to the displacement vector

$$R_T(r) = R_{11}(r\boldsymbol{i}_2) = R_{11}(r\boldsymbol{i}_3) = R_{22}(r\boldsymbol{i}_3) = R_{22}(r\boldsymbol{i}_1) = R_{33}(r\boldsymbol{i}_1) = R_{33}(r\boldsymbol{i}_2). \tag{20}$$

With these definitions we see that the variance of each velocity component is

$$\sigma^2 = R_L(0) = R_T(0). \tag{21}$$

An important quantity is the *integral length scale* L defined as

$$L = \frac{1}{\sigma^2} \int_0^\infty R_L(r) \mathrm{d}\, r. \tag{22}$$

This length characterizes the distance between where the velocity components become uncorrelated.

It is shown by Lumley & Panofsky (1964) in a rather straightforward way that

$$R_T(r) = R_L(r) + \frac{r}{2} \frac{\mathrm{d}R_L}{\mathrm{d}\, r} \tag{23}$$

and that

$$R_{ij}(\boldsymbol{r}) = [R_L(r) - R_T(r)] \frac{r_i r_j}{r^2} + R_T(r)\, \delta_{ij}, \tag{24}$$

where δ_{ij} is Kronecker symbol equal to 1 when the two indices are equal and else 0.

It is often useful to exclude the influence of the large eddies by using the structure-function tensor

$$D_{ij}(\boldsymbol{r}) = \langle (u_i(\boldsymbol{x} + \boldsymbol{r}) - u_i(\boldsymbol{x})(u_j(\boldsymbol{x} + \boldsymbol{r}) - u_j(\boldsymbol{x}) \rangle. \tag{25}$$

This definition implies that

$$D_{ij}(\boldsymbol{r}) = 2[R_{ij}(\boldsymbol{0}) - R_{ij}(\boldsymbol{r})] \tag{26}$$

and

$$D_{ij}(\boldsymbol{r}) = [D_L(r) - D_T(r)] \frac{r_i r_j}{r^2} + D_T(r)\, \delta_{ij}, \tag{27}$$

where, in analogy to (23),

$$D_T(r) = D_L(r) + \frac{r}{2} \frac{\mathrm{d}D_L}{\mathrm{d}\, r} \tag{28}$$

In wave-number space we obtain the spectral velocity tensor by the three-dimensional Fourier transformation

$$\Phi_{ij}(\boldsymbol{k}) = \frac{1}{(2\pi)^3} \int_\infty R_{ij}(\boldsymbol{r})\ \exp(-\mathrm{i}\, \boldsymbol{k} \cdot \boldsymbol{r})\, \mathrm{d}^3 r, \tag{29}$$

where the lower limit ∞ indicates that the integration is taken over the entire space. So we may also write

$$R_{ij}(\boldsymbol{r}) = \int_\infty \Phi_{ij}(\boldsymbol{k})\ \exp(\mathrm{i}\, \boldsymbol{k} \cdot \boldsymbol{r})\, \mathrm{d}^3 k \tag{30}$$

as the inverse transformation.

According to Lumley & Panofsky (1964) the spectral tensor has the form

$$\Phi_{ij}(\boldsymbol{k}) = \frac{E(k)}{4\pi k^2}\left\{\delta_{ij} - \frac{k_i k_j}{k^2}\right\}, \tag{31}$$

where the scalar function $E(k)$ of $k = |\boldsymbol{k}|$ is the energy spectrum.

There are two one-dimensional spectra, the longitudinal and the transversal spectrum, $F_L(k)$ and $F_T(k)$, respectively. They are the counterparts to the covariances $R_L(r)$ and $R_T(r)$ in physical space, defined by (19) and (20), and given by

$$F_L(k) = \frac{1}{2\pi}\int_{-\infty}^{\infty} R_L(r)\,\mathrm{e}^{-\mathrm{i}kr}\mathrm{d}r \tag{32}$$

and

$$F_T(k) = \frac{1}{2\pi}\int_{-\infty}^{\infty} R_T(r)\,\mathrm{e}^{-\mathrm{i}kr}\mathrm{d}r. \tag{33}$$

We see that another way of writing the integral length scale, defined by (22), is

$$L = \frac{\pi F_L(0)}{\sigma^2}. \tag{34}$$

For isotropic turbulence there are the useful relations

$$E(k) = k^3\frac{\mathrm{d}}{\mathrm{d}k}\left\{\frac{1}{k}\frac{\mathrm{d}F_L}{\mathrm{d}\,k}\right\} \tag{35}$$

and, corresponding to)23),

$$F_T(k) = \frac{1}{2}\left\{F_L(k) - k\frac{\mathrm{d}F_L}{\mathrm{d}\,k}\right\}. \tag{36}$$

For small-scale–*locally isotropic*–turbulence with eddies much smaller than L we have

$$F_L(k) = \frac{9}{55}\alpha\varepsilon^{2/3}k^{-5/3} \tag{37}$$

and, by virtue of (36),

$$F_T(k) = \frac{12}{55}\alpha\varepsilon^{2/3}k^{-5/3} \tag{38}$$

where ε is the dissipation rate of specific kinetic energy and where the dimensional constant $\alpha \simeq 1.7$ (Kristensen et al. 1989). Inserting in (35) we get the energy spectrum

$$E(k) = \alpha \varepsilon^{2/3} k^{-5/3}. \tag{39}$$

Since $F_L(k)$ and $F_L(k)$ diverge for $k \to 0$ it is not possible to obtain neither $R_L(r)$ nor $R_L(r)$ by means of the inverse transformation to (32) and (33):

$$R_L(r) = \int_{-\infty}^{\infty} F_L(k)\, \mathrm{e}^{\mathrm{i}kr}\, \mathrm{d}k = 2 \int_0^{\infty} F_L(k)\, \cos(kr)\, \mathrm{d}k \tag{40}$$

and

$$R_T(r) = \int_{-\infty}^{\infty} F_T(k)\, \mathrm{e}^{\mathrm{i}kr}\, \mathrm{d}k = 2 \int_0^{\infty} F_T(k)\, \cos(kr)\, \mathrm{d}k. \tag{41}$$

Of course (40) and (41) are not convergent with the expressions (37) and (38)

The structure functions

$$D_L(r) = 2[R_L(0) - R_L(r)] \tag{42}$$

and

$$D_T(r) = 2[R_T(0) - R_T(r)], \tag{43}$$

characterizing the turbulence without including the large eddies can be determined by means of (40) and (41):

$$D_L(r) = 4 \int_0^{\infty} [1 - \cos(kr)] F_L(k)\, \mathrm{d}k = \frac{27}{55}\, \Gamma\left(\frac{1}{3}\right)\, \alpha\, \varepsilon^{2/3}\, r^{2/3} \tag{44}$$

and

$$D_T(r) = 4 \int_0^{\infty} [1 - \cos(kr)] F_T(k)\, \mathrm{d}k = \frac{36}{55}\, \Gamma\left(\frac{1}{3}\right)\, \alpha\, \varepsilon^{2/3}\, r^{2/3}. \tag{45}$$

If we need to determine $R_L(r)$ or $R_T(r)$ we need to include the variance contributions for the all larger eddies. We may then use the von Kármán spectrum (von Kármán 1948)

$$F_L(k) = \frac{9}{55} \frac{\alpha \varepsilon^{2/3}}{(q^2 + k^2)^{5/6}} \tag{46}$$

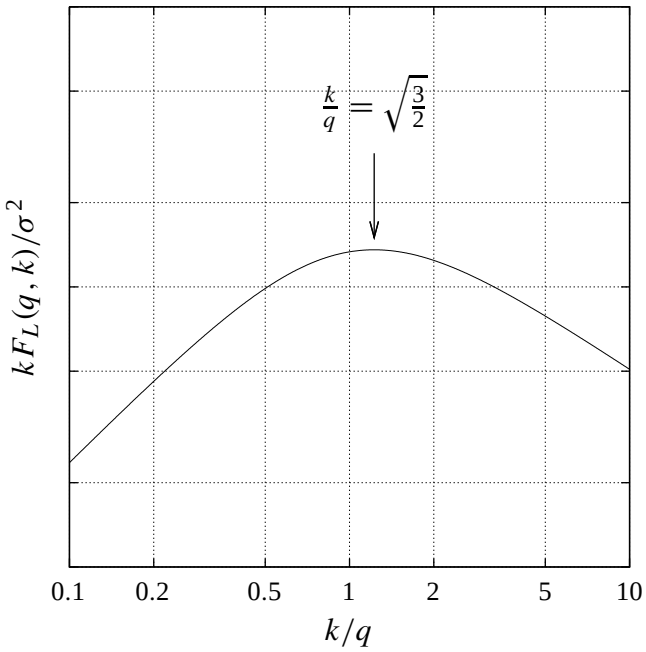

Figure 2: The von Kármán spectrum for the longitudinal velocity component.

for the streamwise velocity component.

Using (36) we see that

$$F_T(k) = \frac{12}{55}\alpha\varepsilon^{2/3}\frac{k^2 + \frac{3}{8}q^2}{(q^2+k^2)^{11/6}} \tag{47}$$

for the transversal velocity component.

Here q is a wave number characterizing the integral turbulence scale. These spectra are practical model expressions used by e.g. ESDU83045 (1983). The form makes some theoretical turbulence analyses quite easy because it contains only one auxiliary parameter q, but is not based on direct experimental evidence. It shows in a qualitative way the spectral behaviour at small wave numbers as illustrated in Fig. 2. The energy spectrum

$$E(k) = \alpha\varepsilon^{2/3}\frac{k^4}{(q^2+k^2)^{17/6}}. \tag{48}$$

is again derived from (46) and (35). In the limit $q = 0$ (46)–(48) become identical to (37)–(39), which of course are of more general validity.

With the von Kármán formulation we get for the one-component variance

$$\sigma^2 = 2\int_0^\infty \frac{9}{55}\frac{\alpha\varepsilon^{2/3}}{(q^2+k^2)^{5/6}}\,\mathrm{d}k = \frac{9}{55}\alpha\varepsilon^{2/3}\frac{B(1/2,1/3)}{q^{2/3}}, \tag{49}$$

where $B(a,b) = \Gamma(a)\Gamma(b)/\,\Gamma(a+b)$ is the beta function. This relation means that we can rewrite (46) and (47) as

$$F_L(k) = \frac{\sigma^2}{B(1/2,1/3)}\frac{q^{2/3}}{(q^2+k^2)^{5/6}} \tag{50}$$

and

$$F_T(k) = \frac{4}{3}\frac{\sigma^2}{B(1/2,1/3)}\frac{q^{2/3}(k^2+\frac{3}{8}q^2)}{(q^2+k^2)^{11/6}}. \tag{51}$$

With the expression (34) for the integral length scale we find by examining (50) the relation

$$Lq = 1/B(1/2,1/3) \approx 0.238. \tag{52}$$

Instead of (44) and (45) we find accordingly

$$D_L(r) = \frac{2\sigma^2}{\Gamma(1/3)}\left\{\Gamma(1/3) - (4qr)^{1/3}K_{1/3}(qr)\right\} \tag{53}$$

and

$$D_T(r) = \frac{2\sigma^2}{\Gamma(1/3)}\left\{\Gamma(1/3) - (4qr)^{1/3}K_{1/3}(qr) + \frac{1}{8}(4qr)^{4/3}K_{2/3}(qr)\right\}. \tag{54}$$

Applying (49) we find that these two last expression are equivalent to (44) and (45) when $qr \ll 1$. When $qr \gg 1$ both $D_L(r)$ and $D_T(r)$ approach $2\sigma^2$ as illustrated by Fig. 3.

We must emphasize that the von Kármán "global" spectral model does not apply to the atmospheric surface layer where the variances of the longitudinal, lateral and vertical velocity components are not the same.

4 Cup Anemometer Dynamics, Phenomenological Model

Figure 4 shows a generic cup rotor with three cups exposed to a wind field with three components, two perpendicular to the anemometer axis, $\widetilde{u}$ and $\widetilde{v}$, and one along the axis $\widetilde{w}$. For convenience we have now changed notation according to $(\widetilde{u}_1, \widetilde{u}_2, \widetilde{u}_3) \Rightarrow (\widetilde{u}, \widetilde{v}, \widetilde{w})$. With the corresponding rate of rotation of the rotor $\widetilde{s}$ (in radians per second) the most general form equation of motion is

$$\dot{\widetilde{s}} \equiv \frac{\mathrm{d}\widetilde{s}}{\mathrm{d}t} = F(\widetilde{s}, \widetilde{h}, \widetilde{w}), \tag{55}$$

where

$$\widetilde{h} = \sqrt{\widetilde{u}^2 + \widetilde{v}^2} \tag{56}$$

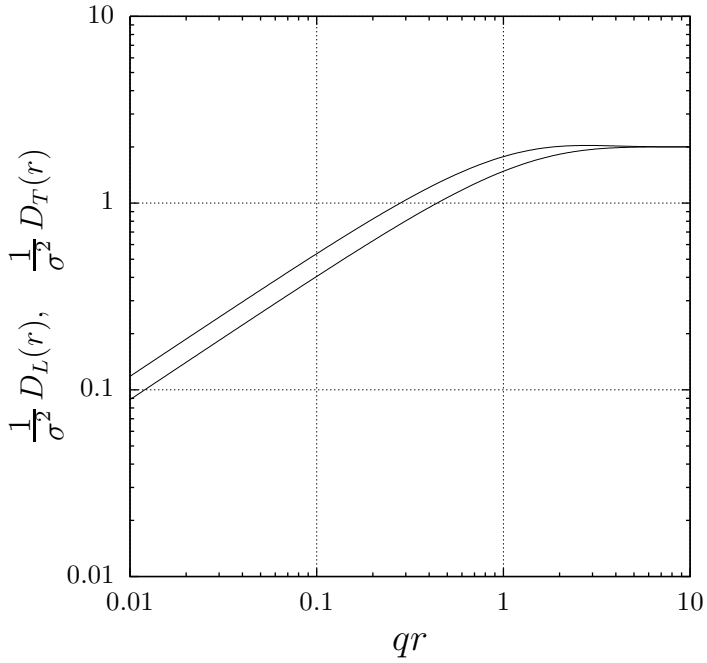

Figure 3: Normalized longitudinal and lateral structure functions. The lower curve shows $D_L(r)/\sigma^2$ and the upper $D_T(r)/\sigma^2$ as they are given by (53) and (54), respectively.

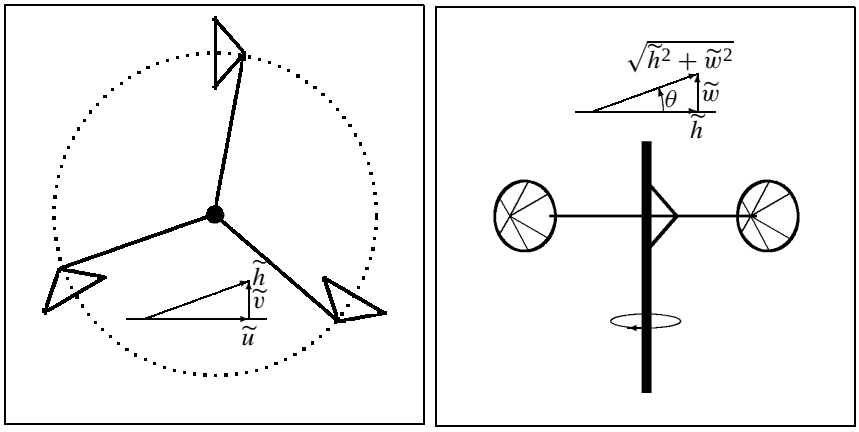

Figure 4: Sketch of a cup-anemometer and indications of the instantaneous wind-velocity components. Left frame: top view. Right frame: side view.

is the total component perpendicular to the axis.

In a constant wind without turbulence (wind tunnel) with $(\widetilde{u}, \widetilde{v}, \widetilde{w}) = (U, 0, 0)$ the rotor will have the constant angular velocity $\widetilde{s} = S$. Inserting into (55), we get

$$0 = F(S, U, 0). \tag{57}$$

This equation defines the calibration which, for a good cup anemometer, can be considered linear, i.e.

$$S = \frac{U - U_\circ}{\ell}, \tag{58}$$

where ℓ is the calibration length and $U_\circ$ the so-called starting speed. This quantity is usually small, about 0.2–0.3 m/s, so in the study of the cup-anemometer dynamics we set $U_\circ$ equal zero. In other words, we replace (58) by

$$\ell S = U, \tag{59}$$

In the turbulent wind field we decompose $\widetilde{s}$ and $(\widetilde{u}, \widetilde{v}, \widetilde{w})$ as follows

$$\begin{Bmatrix} \widetilde{s} \\ \widetilde{u} \\ \widetilde{v} \\ \widetilde{w} \end{Bmatrix} = \begin{Bmatrix} S + s \\ U + u \\ v \\ w \end{Bmatrix}, \tag{60}$$

where U is equal to the mean $\langle \widetilde{u} \rangle$ and S is given by (58). We must assume that $|s| \ll S$, $|u| \ll U$, $|v| \ll U$, and $|w| \ll U$ for the cup anemometer to operate satisfactorily. An immediate consequence of this assumption is that to second order we have

$$\begin{aligned} \widetilde{h} &= \sqrt{(U+u)^2 + v^2} = U \left(1 + 2\frac{u}{U} + \frac{u^2 + v^2}{U^2}\right)^{1/2} \\ &\simeq U \left(1 + \frac{1}{2}\left(2\frac{u}{U} + \frac{u^2 + v^2}{U^2}\right) + \frac{(1/2) \times (-1/2)}{2} \left(2\frac{u}{U}\right)^2\right) = U + u + \frac{v^2}{2U} \end{aligned} \tag{61}$$

Initially we simplify the model by considering only a horizontally fluctuating wind, i.e. $\widetilde{w} = 0$. The dynamic equation (55) reduces to

$$\dot{\widetilde{s}} = F(\widetilde{s}, \widetilde{h}, 0) \equiv G(\widetilde{s}, \widetilde{h}) \tag{62}$$

and (57) to

$$0 = G(S, U). \tag{63}$$

Expanding (62) to second order in s, u, and v, we get

$$\begin{aligned}\dot{s} &= \underbrace{G(S,U)}_{=0} + \frac{\partial G}{\partial S}s + \frac{\partial G}{\partial U}\left(u + \frac{v^2}{2U}\right) \\ &\quad + \frac{1}{2}\left(\frac{\partial^2 G}{\partial S^2}s^2 + 2\frac{\partial^2 G}{\partial S \partial U}su + \frac{\partial^2 G}{\partial U^2}u^2\right). \end{aligned} \tag{64}$$

All the first and second derivatives are taken at the point (S, U). Neglecting first the second-order terms, we see that (64) becomes the equation for a first-order, linear filter. Since the solution must be finite, we infer that $\partial G/\partial S$ must be negative. In fact, this derivative determines the filter time-constant $\tau_\circ$ by

$$\frac{1}{\tau_\circ} = -\frac{\partial G}{\partial S}. \tag{65}$$

The function $G(S, U)$ is almost entirely determined by the wind drag force on the rotor and is therefore proportional to the air density ϱ multiplied by a second-order polynomial in S and U. We see then, with the aid of (19), that the definition (65) of $\tau_\circ$ implies that this quantity is inversely proportional to $\varrho \times U$. It means that the distance

$$\ell_\circ = U\tau_\circ \tag{66}$$

is independent of the wind speed. We have here introduced the distance constant which, apart from its dependence of the air density, can be considered an instrument constant, in contrast to the time constant τ.

Differentiating (63), we obtain with the aid of (59)

$$0 = \frac{\partial G}{\partial S}\frac{\mathrm{d}S}{\mathrm{d}U} + \frac{\partial G}{\partial U} = \frac{1}{\ell}\frac{\partial G}{\partial S} + \frac{\partial G}{\partial U}, \tag{67}$$

so that

$$\frac{\partial G}{\partial U} = \frac{1}{\ell\tau_\circ}. \tag{68}$$

The first-order filter function can thus be written

$$\dot{s} + \frac{s}{\tau_\circ} = \frac{u}{\ell\tau_\circ}. \tag{69}$$

It is a useful consequence of (69) that there is a relation between the variance $\langle \dot{s}^2 \rangle$ and the covariance $\langle su \rangle$. This can be seen by multiplying (69) by s and then taking the average. We use the fact that for the stationary time series s the mean and higher order moments are independent of time, i.e.

$$\left\langle s\frac{\mathrm{d}s}{\mathrm{d}t}\right\rangle = \frac{1}{2}\frac{\mathrm{d}}{\mathrm{d}t}\langle s^2\rangle = 0. \tag{70}$$

In other words,

$$\langle s^2 \rangle = \frac{\langle su \rangle}{\ell}. \tag{71}$$

Rewriting (64) in the form

$$\dot{s} + \frac{s}{\tau_\circ} = \frac{u}{\ell \tau_\circ} + \frac{1}{2}\left(\frac{\partial^2 G}{\partial S^2} s^2 + 2 \frac{\partial^2 G}{\partial S \partial U} su + \frac{\partial^2 G}{\partial U^2} u^2 \right) + \frac{v^2}{2U\ell\tau_\circ}, \tag{72}$$

we can now determine the bias on the measured wind speed by taking the mean of (72). Since u is the fluctuation around the mean U, $\langle u \rangle$ is zero by definition. The mean $\langle s \rangle$ is of course constant, so that $\langle \dot{s} \rangle = 0$, but $\langle s \rangle$ is not zero, because S is only the mean of the rotation rate $\widetilde{s}$ when there is no turbulence. In fact, the dimensionless quantity $\langle s \rangle / S$ is the relative bias on the measured wind speed. From (72) we get

$$\frac{\langle s \rangle}{S} = \frac{\tau_\circ}{2S} \left\{ \frac{\partial^2 G}{\partial S^2} \langle s^2 \rangle + 2 \frac{\partial^2 G}{\partial S \partial U} \langle su \rangle + \frac{\partial^2 G}{\partial U^2} \langle u^2 \rangle \right\} + \frac{\langle v^2 \rangle}{2U^2}. \tag{73}$$

Just like we obtained (67), we derive a relation between the second derivatives by differentiating (63) twice with respect to U. The result is

$$\frac{1}{\ell^2} \frac{\partial^2 G}{\partial S^2} + \frac{2}{\ell} \frac{\partial^2 G}{\partial S \partial U} + \frac{\partial^2 G}{\partial U^2} = 0. \tag{74}$$

With this equation and (71), we reformulate (73):

$$\frac{\langle s \rangle}{S} = \frac{\ell \tau_\circ}{2U} \frac{\partial^2 G}{\partial U^2} \{ \langle u^2 \rangle - \ell \langle su \rangle \} + \frac{\langle v^2 \rangle}{2U^2}. \tag{75}$$

We need to determine the coefficient $\ell \tau_\circ / (2U) \times \partial^2 G / \partial U^2$. Fortunately, this has been done by Wyngaard et al. (1974) and by Coppin (1982) in rather sophisticated wind-tunnel experiments. Their results are summarized by Kristensen (1998) and for a number of widely different types of cup anemometers they found that within about 10%

$$\frac{\ell U \tau_\circ}{2} \frac{\partial^2 G}{\partial U^2} = 1, \tag{76}$$

independent of the mean-wind speed U. We will assume that this instrument constant, which was originally called a_4 by Wyngaard et al. (1974), is one and, consequently, that (75) becomes

$$\frac{\langle s \rangle}{S} = \frac{1}{U^2} \{ \langle u^2 \rangle - \ell \langle su \rangle \} + \frac{\langle v^2 \rangle}{2U^2}. \tag{77}$$

To evaluate $\ell\langle su\rangle$ we need to find out how $s = s(t)$ depends on $u = u(t)$. We find the relation by solving (69). The solution is

$$s(t) = \frac{1}{\ell}\int_0^\infty u(t-\tau)\,\mathrm{e}^{-\tau/\tau_\circ}\,\frac{\mathrm{d}\tau}{\tau_\circ}. \tag{78}$$

This leads to

$$\begin{aligned}\langle u^2\rangle - \ell\langle su\rangle &= \langle u^2\rangle - \left\langle \int_0^\infty u(t)u(t-\tau)\,\mathrm{e}^{-\tau/\tau_\circ}\,\frac{\mathrm{d}\tau}{\tau_\circ}\right\rangle \\ &= \int_0^\infty \langle u^2 - u(t)u(t-\tau)\rangle\,\mathrm{e}^{-\tau/\tau_\circ}\,\frac{\mathrm{d}\tau}{\tau_\circ} \\ &= \frac{1}{2}\int_0^\infty \left\langle [u(t-\tau)-u(t)]^2\right\rangle\,\mathrm{e}^{-\tau/\tau_\circ}\,\frac{\mathrm{d}\tau}{\tau_\circ}.\end{aligned} \tag{79}$$

The quantity average $\langle[u(t-\tau)-u(t)]^2\rangle$ is the longitudinal structure function (42) which, for stationary signals like $u(t)$, depends on the time difference τ and is independent of the absolute time t (Lumley & Panofsky 1964, page 46).

$$D_L(r) = \left\langle \left[u\left(\frac{x-r}{U}\right) - u\left(\frac{x}{U}\right)\right]^2\right\rangle, \quad x = Ut. \tag{80}$$

Thus we may write (42) in the form

$$\langle u^2\rangle - \ell\langle su\rangle = \frac{1}{2}\int_0^\infty D_L(r)\,\mathrm{e}^{-r/\ell_\circ}\,\frac{\mathrm{d}r}{\ell_\circ}, \tag{81}$$

where we have changed integration variable from τ to r and where we have used the relation (66) between the length constant $\ell_\circ$ and the time constant $\tau_\circ$. Inserting in (77) the bias δU due to the horizontal velocity velocity fluctuations is therefore given by

$$\frac{\delta U}{U} = \frac{\langle s\rangle}{S} = \frac{1}{2U^2}\int_0^\infty D_L(r)\,\mathrm{e}^{-r/\ell_\circ}\,\frac{\mathrm{d}r}{\ell_\circ} + \frac{\langle v^2\rangle}{2U^2}. \tag{82}$$

The result (82) would be the final result concerning the bias on the mean-wind speed if the cup anemometer angular response were ideal in the sense that only the wind component perpendicular to the rotor axis exerts

a forcing on the rotor. In this case we say that the anemometer has a cosine angular response. The angular response $g(\theta)$ is usually not a cosine. In general we have

$$g(\theta) = \cos\theta + \mu_1 \sin\theta + \mu_2(1 - \cos\theta), \tag{83}$$

where μ_1 and μ_2 are dimensionless instrument constants. For small angles this becomes to second order in θ

$$g(\theta) \simeq 1 + \mu_1\theta - (1 - \mu_2)\frac{\theta^2}{2}, \tag{84}$$

showing that μ_1 characterizes the angular skewness or up/down asymmetry while μ_2 defines the curvature. If $\mu_1 = \mu_2 = 0$ the angular response is a cosine response. If $\mu_1 = 0$ and $\mu_2 = 1$ the angular response is flat while $\mu_2 < 0$ means that $g(\theta)$ falls below the ideal $\cos\theta$.

This means that the forcing on the cup rotor is no longer determined by (61), but rather by

$$\widetilde{h}' = \sqrt{\widetilde{h}^2 + \widetilde{w}^2}\, g(\theta). \tag{85}$$

To second order in the perturbing quantities we get, in analogy to (61),

$$\sqrt{\widetilde{h}^2 + \widetilde{w}^2} = \sqrt{(U+u)^2 + v^2 + w^2} \simeq U + u + \frac{v^2 + w^2}{2U}, \tag{86}$$

so that

$$\cos\theta = \frac{\widetilde{h}}{\sqrt{\widetilde{h}^2 + \widetilde{w}^2}} \simeq 1 - \frac{w^2}{2U^2} \tag{87}$$

and

$$\sin\theta = \frac{\widetilde{w}}{\sqrt{\widetilde{h}^2 + \widetilde{w}^2}} \simeq \frac{w}{U} - \frac{uw}{U^2}. \tag{88}$$

Inserting (87) and (88) into (83), the expression for the "apparent" horizontal velocity component becomes

$$\widetilde{h}' = U + (u + \mu_1 w) + \frac{v^2 + \mu_2 w^2}{2U}. \tag{89}$$

In other words, $\widetilde{h}'$ is given by $\widetilde{h}$ if we make the replacements

$$\begin{array}{rcl} u & \Rightarrow & u + \mu_1 w \\ v^2 & \Rightarrow & v^2 + \mu_2 w^2. \end{array} \tag{90}$$

This implies that (79) is still valid with the replacement

$$\begin{aligned}\left\langle [u(t-\tau)-u(t)]^2 \right\rangle \;&\Rightarrow\; \left\langle [\{u(t-\tau)+\mu_1 w(t-\tau)\}-\{u(t)+\mu_1 w(t)\}]^2 \right\rangle \\ &= \underbrace{\left\langle [u(t-\tau)-u(t)]^2 \right\rangle}_{=D_L(U\tau)} + \mu_1^2 \underbrace{\left\langle [w(t-\tau)-w(t)]^2 \right\rangle}_{=D_T(U\tau)} \\ &\quad + 2\mu_1 \underbrace{\langle [u(t-\tau)-u(t)][w(t-\tau)-w(t)] \rangle}_{=0}. \end{aligned} \tag{91}$$

Under each of the three terms we have given their values according to general rules (24)—(28) for isotropic turbulence.

With the replacements (90) the complete bias expression becomes, as a generalization of (82),

$$\frac{\delta U}{U} = \frac{\langle s \rangle}{S} = \frac{1}{2U^2} \int_0^\infty D_L(r)\, \mathrm{e}^{-r/\ell_\circ} \frac{\mathrm{d}r}{\ell_\circ} + \frac{\mu_1^2}{2U^2} \int_0^\infty D_T(r)\, \mathrm{e}^{-r/\ell_\circ} \frac{\mathrm{d}r}{\ell_\circ} + \frac{\langle v^2 \rangle + \mu_2 \langle w^2 \rangle}{2U^2}. \tag{92}$$

To include the imperfect angular response we must also apply the replacement (90) to the first-order equation (69), which then becomes

$$\dot{s} + \frac{s}{\tau_\circ} = \frac{u + \mu_1 w}{\ell \tau_\circ}. \tag{93}$$

This equation describes a first-order, low-pass filtering of the signal $u(t) + \mu_1 w(t)$ with the time constant $\tau_\circ = \ell_\circ / U$. We note that the parameter μ_2 does only enter here if second-order perturbations are included.

5 Overspeeding in the Atmospheric Surface Layer

The cup-anemometer is usually operated at altitudes of 10 m or more and, consequently, the integral scale of the turbulence will be larger than 50 m (Kristensen et al. 1989). Comparing this scale with the distance constant $\ell_\circ$ which is seldom more than a few meters, we may safely assume that the the turbulence is close to being locally isotropic. This means that we may apply (44) and (45) for $D_L(r)$ and $D_T(r)$ in (92).

The first two terms on the right-hand side of (85) become

$$\frac{1}{2U^2} \int_0^\infty D_L(r)\, \mathrm{e}^{-r/\ell_\circ} \frac{\mathrm{d}r}{\ell_\circ} = \frac{6\sqrt{3}\pi}{55}\, \alpha\, \frac{(\varepsilon \ell_\circ)^{2/3}}{U^2} \tag{94}$$

and

$$\frac{\mu_1^2}{2U^2} \int_0^\infty D_T(r)\, \mathrm{e}^{-r/\ell_\circ} \frac{\mathrm{d}r}{\ell_\circ} = \frac{8\sqrt{3}\pi}{55}\, \alpha\, \mu_1^2\, \frac{(\varepsilon \ell_\circ)^{2/3}}{U^2}. \tag{95}$$

The resulting relative bias can now be written

$$\frac{\delta U}{U} = \frac{6\sqrt{3}\pi}{55}\,\alpha\,\left(1+\frac{4}{3}\mu_1^2\right)\frac{(\varepsilon\ell_\circ)^{2/3}}{U^2} + \frac{\langle v^2\rangle + \mu_2\langle w^2\rangle}{2U^2}. \tag{96}$$

When $U \gtrsim 5$ m/s the surface layer can be considered neutrally stratified and the vertical velocity gradient is then given by

$$\frac{\mathrm{d}U}{\mathrm{d}z} = \frac{u_*}{\kappa z}, \tag{97}$$

where $\kappa \simeq 0.4$ is the von Kármán constant and

$$u_* = \sqrt{-uw} \tag{98}$$

the friction velocity. The relation between u_* and the dissipation is

$$\varepsilon = \frac{u_*^3}{\kappa z}. \tag{99}$$

Consequently, we may reformulate (96) as follows

$$\frac{\delta U}{U} = \underbrace{\frac{6\sqrt{3}\pi}{55}\,\alpha}_{\simeq 1.01}\,\left(1+\frac{4}{3}\mu_1^2\right)\frac{u_*^2}{U^2}\left(\frac{\ell_\circ}{\kappa z}\right)^{2/3} + \frac{\langle v^2\rangle + \mu_2\langle w^2\rangle}{2U^2}. \tag{100}$$

This equation can also be expressed in terms of the longitudinal variance $\langle u^2\rangle$ instead of the friction velocity u_* squared. According to Panofsky & Dutton (1984) we have the empirical relation

$$\frac{\langle u^2\rangle^{1/2}}{u_*} \simeq 2.39 \pm 0.03 \tag{101}$$

in flat terrain and with neutral stratification. We obtain the practical formulation

$$\frac{\delta U}{U} \simeq 0.325\,\left(1+\frac{4}{3}\mu_1^2\right)\frac{\langle u^2\rangle}{U^2}\left(\frac{\ell_\circ}{z}\right)^{2/3} + \frac{\langle v^2\rangle + \mu_2\langle w^2\rangle}{2U^2}. \tag{102}$$

6 Overspeeding in a Wind Tunnel

The length scale Δ in a wind tunnel is small compared to that of the atmosphere and to quantify the bias we assume that the turbulence is isotropic. The longitudinal spectrum (40) is displayed in Fig. 2 in the usual "area conserving" form. In this case the three component variances are all the same, namely

$$\sigma^2 = \langle u^2\rangle = \langle v^2\rangle = \langle w^2\rangle. \tag{103}$$

We may now write (92 in the form

$$\frac{\delta U}{U} = \frac{\sigma^2}{U^2}\left[\varphi_L(q\ell_\circ) + \mu_1^2\varphi_T(q\ell_\circ)\right] + \frac{(1+\mu_2)\sigma^2}{2U^2}, \tag{104}$$

where

$$\begin{aligned}\varphi_L(q\ell_\circ) &= \frac{1}{2\sigma^2}\int_0^\infty D_L(r)\,\mathrm{e}^{-r/\ell_\circ}\,\frac{\mathrm{d}r}{\ell_\circ} \\ &= 1 + \frac{B(2/3,5/6)}{2}\frac{(q\ell_\circ)^{2/3}}{(1-(q\ell_\circ)^2)^{5/6}} - {}_2F_1(1/2,1;2/3;(q\ell_\circ)^2)\end{aligned} \tag{105}$$

and

$$\begin{aligned}\varphi_T(q\ell_\circ) &= \frac{1}{2\sigma^2}\int_0^\infty D_T(r)\,\mathrm{e}^{-r/\ell_\circ}\,\frac{\mathrm{d}r}{\ell_\circ} \\ &= 1 + \frac{B(2/3,5/6)}{2}\frac{(q\ell_\circ)^{2/3}}{(1-(q\ell_\circ)^2)^{5/6}} - {}_2F_1(1/2,1;2/3;(q\ell_\circ)^2) \\ &+ \frac{2-12(q\ell_\circ)^2+[2+3(q\ell_\circ)^2][B(1/2,2/3)(q\ell_\circ)^2 2/3(1-(q\ell_\circ)^2)^{1/6} - {}_2F_1(-1/2,1;2/3;(q\ell_\circ)^2)]}{18(1-(q\ell_\circ)^2)}.\end{aligned} \tag{106}$$

These two functions can be determined in terms of the hypergeometric function (Oberhettinger 1964) with the expressions (53) and (54). They are presented in Fig. 5.

7 Summary

A good cup anemometer is an attractive instrument for practical purposed, mainly because it is omnidirectional and easy to deploy in the atmospheric boundary layer. It can safely be assumed to have a linear calibration, often presented as

$$U = A_\circ + B_\circ \times f, \tag{107}$$

where $A_\circ$ and $B_\circ$ are independent of the wind speed. The first is called the "starting threshold". The quantity f is the frequency in Hz which is proportional to the rotation rate of the rotor S in rad/s. Since this frequency, in turn, is proportional to the number of pulses n created per one full revolution,we have

$$f = n \times \frac{S}{2\pi}.$$

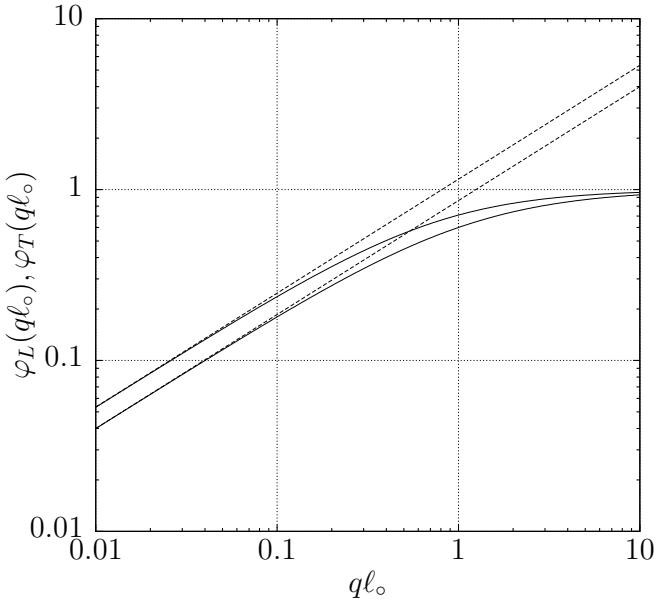

Figure 5: The functions $\varphi_L(q\ell_\circ)$ and $\varphi_T(q\ell_\circ)$, based on the von Kármán spectrum. For values of $q\ell_\circ$ up to about 0.1 we are in the domain of local isotropy, where both functions are proportional to $(q\ell_\circ)^{2/3}$.

In the preceding considerations the linearity is presented by (58):

$$S = \frac{U - U_\circ}{\ell},$$

where S is the cup rotation-rate in rad/s and $U_\circ$ is the "starting speed" and ℓ the "calibration length". Obviously, $U_\circ = A_\circ$, and the relation between ℓ and $B_\circ$ becomes

$$\ell = n \times \frac{B_\circ}{2\pi}$$

in terms of the number n of pulses being created in one revolution of the cup rotor. The calibration length ℓ can be interpreted as the length of the column air which has for blow through the anemometer for the rotor to complete one full rotation i.e. 360°.

The cup anemometer is always mounted with vertical axis and since we assume that the mean wind direction is perpendicular to the axis. However, the fluctuation wind velocity components (with the mean-wind vector removed) can have any direction. Figure 4 shows the instantaneous velocity components $(\widetilde{u}, \widetilde{v}, \widetilde{w})$ and the total horizontal velocity component $\widetilde{h} = \sqrt{\widetilde{u}^2 + \widetilde{v}^2}$ in relation to the cup-anemometer rotor. As the right-hand frame shows the magnitude of the wind vector is $\sqrt{\widetilde{h}^2 + \widetilde{w}^2}$ and if the response were ideal, the anemometer would respond to $\sqrt{\widetilde{h}^2 + \widetilde{w}^2}\cos\theta$, where $\tan\theta = \widetilde{w}/\widetilde{h}$. In other words, the vertical velocity will then not influence the angular speed of the rotor. However, cup anemometers are not ideal so in general they will respond to the more general form, $\sqrt{\widetilde{h}^2 + \widetilde{w}^2}\, g(\theta)$. The function $g(\theta)$ is the so-called angular response. We find that for small angles we can use the equation

$$g(\theta) = 1 + \mu_1\theta - (1 - \mu_2)\frac{\theta^2}{2}.$$

This expression has two parameter μ_1, which account for the up-down asymmetry, and μ_2, which describes the curvature. We see that if μ_1 the response is symmetric. In this case $\mu_2 = 0$ means that the angular becomes ideal, while $\mu_2 = 0$ implies that the angular response is flat.

The dynamics of the cup anemometer can be described as a first-order filter in the fluctuating velocity components and the fluctuating angular velocity s of the cup rotor:

$$\dot{s} + \frac{s}{\tau_\circ} = \frac{u + \mu_1 w}{\ell \tau_\circ}.$$

If, at a given wind speed with constant rotation rate, a sudden increase in the wind speed will cause the rotor to increase the rotation rate until the new equilibrium is obtained. For a first order filter τ is the time it takes to obtain 63 percent of the new equilibrium. The distance constant is defined by

$$\ell_\circ = U \tau_\circ$$

This is a true instrument constant and can be interpreted as the length of the column of air which must pass through the rotor to obtain 63 percent of the final equilibrium rotation rate.

So a cup anemometer is characterized by five constants: 1) One velocity $U_\circ$, the starting threshold. 2) Two lengths, the calibration length ℓ and the distance constant $\ell_\circ$. 3) Two dimensionless constants, μ_1 and μ_2 describing the angular response.

We have the tools to determine the overspeeding. For the neutral atmospheric surface layer we have

$$\frac{\delta U}{U} \simeq 0.325 \left(1 + \frac{4}{3}\mu_1^2\right) \frac{\langle u^2 \rangle}{U^2} \left(\frac{\ell_\circ}{z}\right)^{2/3} + \frac{\langle v^2 \rangle + \mu_2 \langle w^2 \rangle}{2U^2}$$

expressed in terms of the mean-wind speed U, the three velocity variances ($\langle u^2 \rangle$, $\langle v^2 \rangle$, $\langle w^2 \rangle$), and the measuring height z.

In the wind tunnel the bias will depend on the linear dimension of the tunnel and the distance constant. Inspection of (104) and Fig. 5 seem to indicate that the relative overspeeding i about the squared turbulence intensity.

References

Busch, N. E. & Kristensen, L. (1976), 'Cup anemometer overspeeding', *J. Appl. Meteor.* **15**, 1328–1332.

Coppin, P. A. (1982), 'An examination of cup anemometer overspeeding', *Meteorol. Rdsch.* **35**, 1–11.

ESDU83045 (1983), *Strong Winds in the Atmospheric Boundary Layer. Part 2: Discrete Gust Speeds*, Engineering Science Data Unit, Ltd.

Kaganov, E. I. & Yaglom, A. M. (1976), 'Errors in wind speed measurements by rotation anemometers', *Boundary-Layer Meteorol.* **10**, 1–11.

Kristensen, L. (1993), The cup anemometer and other exciting instruments, Technical Report R-615(EN), Risø National Laboratory.

Kristensen, L. (1998), 'Cup anemometer behavior in turbulent environments', *J. Atmos. Ocean. Technol.* **15**, 5–17.

Kristensen, L. (1999), 'The perennial cup anemometer', *Wind Energy* **2**, 59–75.

Kristensen, L., Lenschow, D. H., Kirkegaard, P. & Courtney, M. S. (1989), 'The spectral velocity tensor for homogeneous boundary-layer turbulence', *Boundary-Layer Meteorol.* **47**, 149–193.

Lumley, J. L. & Panofsky, H. A. (1964), *The Structure of Atmospheric Turbulence*, John Wiley & Sons, Inc., New York.

Middleton, W. E. K. (1969), *Invention of Meteorological Instruments*, The Johns Hopkins Press, Baltimore, MD.

Oberhettinger, F. (1964), Hypergeometric functions, *in* M. Abramowitz & I. Stegun, eds, 'Handbook of Mathematical Functions with Formulas, Graphs, and Mathematical Tables. Gamma Function and Related Functions', Applied Mathematics Series 55, National Bureau of Standards, chapter 13, pp. 555–566.

Panofsky, H. A. & Dutton, J. A. (1984), *Atmospheric Turbulence: Models and Methods for Engineering Applications*, John Wiley & Sons, Inc., New York.

Patterson, J. (1926), 'The cup anemometer', *Trans. Roy. Soc. Canada, Ser. III* **20**, 1–54.

Schrenk, O. (1929), 'Über die Trägheitsfehler des Schalenkreuz-Anemometers bei schwankender Windstärke', *Z. Tech. Phys.* **10**, 57–66.

von Kármán, T. (1948), 'Progress in the statistical theory of turbulence', *Proc. Nat. Acad. Sci.* **34**, 530–539.

Wyngaard, J. C. (1981), 'Cup, propeller, vane, and sonic anemometers in turbulence research', *Ann. Rev. Fluid Mech.* **13**, 399–423.

Wyngaard, J. C., Bauman, J. T. & Lynch, R. A. (1974), Cup anemometer dynamics, *in* 'Proc. Flow, Its Measurements and Control in Science and Industry', Vol. 1, Instrument Society of America, Pittsburg, PA, pp. 701–708.